Mechanistic Models for LAH Reductions of Acetonitrile and Malononitrile. Aggregation Effects of Li+ and AlH3 on Imide–Enamide Equilibria

Rainer Glaser,* Laura Ulmer, and Stephanie Coyle

Department of Chemistry, University of Missouri, Columbia, Missouri 65211, United States

S Supporting Information

ABSTRACT: The results are reported of an ab initio study of the addition of $LiAlH_4$ to acetonitrile and malononitrile at the MP2(full)/6-311+G* level considering the effects of electron correlation at higher levels up to QCISD(T)/6-311++G-(2df,2pd) and including ether solvation. All imide ($RCH_2CH=N^-$) and enamide ($RCH^-CH=NH \leftrightarrow RCH=CHN^-H$) adducts feature strong interactions between the organic anion and both Li+ and AlH_3. The relative stabilities of the tautomeric LAH adducts are compared to the tautomer preference energies of the LiH adducts and of the hydride adducts of the nitriles. Alane affinities were determined for the lithium ion pairs formed by LiH addition to the nitriles. The results show that alane binding greatly affects the imide–enamide equilibria and that alane complexation might even provide a thermodynamic preference for the imide intermediate. While lithium enamides of malononitrile are much more stable than lithium imides, alane binding dramatically reduces the enamide preference so that both tautomers are present at equilibrium. Implications are discussed regarding to the propensity for multiple hydride reductions and with regard to the mechanism of reductive nitrile dimerization. A detailed mechanism is proposed for the formation of 2-aminonicotinonitrile (**2ANN**) in the LAH reduction of malononitrile.

Imide ⇌ Enamide ⟶ 2ANN
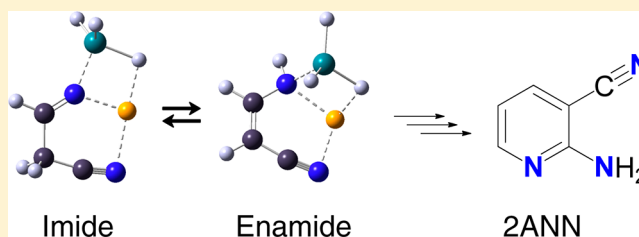
INTRODUCTION

The reduction of nitriles[1,2] by lithium aluminum hydride (LAH) was first investigated in the 1950s by Amundsen[3] and by Soffer and Katz.[4,5] Typically, a small excess of LAH was reacted with the nitrile to afford primary amines after aqueous workup (Scheme 1). The reaction was thought to involve two hydride additions that result in aggregates first of the imide anion (i.e., $R'HC=N^-$) and then of amide dianion (i.e., $R'CH_2N^{2-}$). Imines and aldehydes are side products formed by hydrolysis of the imide aggregate. Soffer and Katz studied a variety of nitriles RCN (R = C_3H_7 (n-butyro), C_5H_{11} (n-capro), CH_2Ph (phenylaceto), Ph (benzo), MePh (o-toluo)) and also observed large amounts of diamine dimers in the reduction of primary nitriles (Scheme 1).

In 1969, Sieveking and Lüttke reported that the LAH reduction of malononitrile, $H_2C(CN)_2$ produces enamino nitriles.[6] Equimolar amounts of malononitrile and LAH were reacted at room temperature and subsequently washed with water and NaOH to yield a mixture of *cis*- and *trans*-3-aminoacrylonitrile (**3AAN**) as the major product in about 90% yield and the byproduct 2-aminonicotinonitrile (**2ANN**) in about 7% yield (Scheme 2). The formation of **2ANN** was confirmed by its independent synthesis in 75–79% by treatment of 2-chloronicotinonitrile with ammonia.[7] In 1974, Brown and Ienega[8,9] also prepared and characterized **3AAN** by LAH reduction of malononitrile and, in addition, reported the alternative synthesis of **3AAN** by heating isoxazole with ethanolic ammonia in 31% yield. In 2005, another alternative

for the synthesis of **3AAN** was reported by Guillemin et al.[10] via NH_3 addition to cyanoacetylene, $HC≡C–C≡N$, in chloroform or gas phase. The Guillemin synthesis affords **3AAN** in 80% overall yield with a (*Z*)/(*E*) ratio of 1:1, and the (*Z*)/(*E*) ratio increases to 20 after distillation (ΔG_{exp} = 1.8 kcal/mol) in agreement with computed isomer preferences.[11,12]

We came across this nitrile reduction chemistry because of our interest in the chemistry of **3AAN**.[13,14] In particular, we were wondering what might cause the greatly different outcomes in the LAH reductions of alkyl nitriles and malononitrile. Alkyl nitriles are reduced all the way to amines (two hydride additions) or diamines (three hydride additions and one carbanion addition). On the other hand, all products of the LAH reduction of malononitrile are products of just one hydride addition. In particular, the formation of **2ANN** formally requires one hydride addition, one C–C bond formation, one C–N bond formation, and one N-loss. The formation of diamine dimers shows that enamide formation is possible for primary alkyl nitriles and, hence, the increased acidity of malononitrile alone does not explain the different product palettes.

Here we report the results of an ab initio study of the addition of LAH (**1**, lithium aluminum hydride) to acetonitrile **2** and malononitrile **6**. The study of the LAH reduction of **2**

Scheme 1. LAH Reduction of Nitriles Leads to Amines and Diamine Dimers[a]
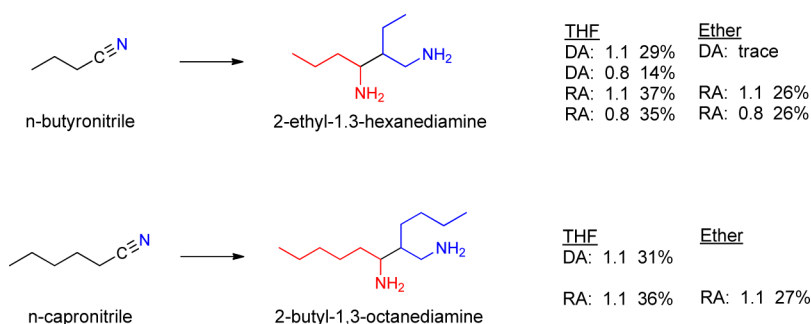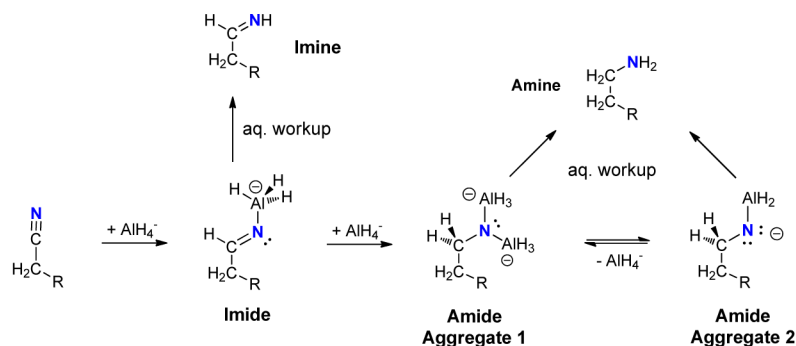
[a]Yields are provided for diamines formed by direct addition (DA) and reverse addition (RA) in THF and ether.

Scheme 2. LAH Reduction of Malononitrile Leads to 3-Aminoacrylonitrile (3AAN) and 2-Aminonicotinonitrile (2ANN)

includes isomers of imide **3** and of coordination isomers **4** (alane at N) and **5** (alane at C) of the enamide tautomer. The study of LAH reduction of **6** considered the respective isomers of imide **7** and isomers of the coordination isomers **8** and **9** of the enamide tautomer. All adducts feature strong interactions between the organic anion and both Li^{+} and AlH$_3$ as well as interactions between the Lewis acids (i.e., Li^{+}···HAlH$_2$). To assess the strengths of alane binding in the LAH adducts, alane affinities were determined for the lithium ion pairs formed by LiH addition to acetonitrile (imide **19**, enamide **20**) and malononitrile (imide **21**, enamide **22**). The results show that alane binding dramatically affects the imide-enamide equilibria. While lithium enamides are *much more* stable than lithium imides, alane binding greatly reduces the tautomer preference so that both tautomers are present at equilibrium and complexation might even favor the imide intermediate. Implications are discussed with regard to the propensity for multiple hydride reductions of a nitrile and with regard to the mechanism of reductive nitrile dimerization. A detailed mechanism is proposed for the formation of **2ANN** in the LAH reduction of malononitrile and it is hoped that this mechanism might lead to improved syntheses of 2-amino-nicotinonitrile[15] and syntheses of other pyridines.[16]

■ COMPUTATIONAL METHODS

Second-order Møller–Plesset perturbation theory (MP2) was employed for the potential energy surface analysis[17−20] in conjunction with the 6-311+G* basis set,[21] MP2(full)/6-311+G*, to locate and characterize stationary structures. Correlated electronic structure methods are required to account for dispersion and, in particular, for the adequate description of dative bonding. Single point energies were computed for selected systems with the QCISD(full,T) method[22] and the extended basis set[23] 6-311++G(2df,2dp). Multilevel methods[24] such as Gn[25] and CBS[26] approximate such high levels with complex series of lower level computations and the results are thought to match experiment to about 1−2 kcal/mol. Solvation can be modeled by continuous[27,28] and discrete solvent models,[29] and we employed the recently developed solvation model density (SMD) method,[30,31] a density-based, self-consistent reaction field theory of bulk electrostatics (SCRF), to assess solvation effects on selected isomer preference energies. The SMD method accounts for long-range electrostatic polarization (bulk solvent) and also for short-range effects associated with cavitation, dispersion, and solvent structural effects (CDS). Computations were performed with Gaussian09[32] in conjunction with Gaussview 5[33] on an SGI Altix BX2 SMP system with 64 Itanium2 processors and a Dell EM64T cluster system with 512 processors.

Cartesian coordinates of all optimized structures are provided as Supporting Information, selected structural parameters are collected in Table 1, and molecular models are shown in the figures. Total energies (E_{tot}), vibrational zero point energies (VZPE), thermal energies (TE), molecular entropies (S), the numbers of imaginary frequencies (NI), and the lowest vibrational frequencies ν_1 and ν_2 are given in Table S1 of the Supporting Information. In Table 2 are listed pertinent relative and reaction energies (in kcal/mol) and four thermodynamic values are provided for each parameter, and these are ΔE, $\Delta H_0 = \Delta E + \Delta \text{VZPE}$, $\Delta H_{298} = \Delta E + \Delta \text{TE} + \Delta(pV)$, and $\Delta G_{298} = \Delta H_{298} + 298.15 \Delta S$. We are interested in condensed-phase chemistry, and $\Delta(pV)$ is assumed to be negligible.

Table 1. Selected Structural Parameters[a]

	$d(CN)$	$d(CC)$	$d(N\cdots Li)$	$d(N\cdots Al)$	$d(C\cdots Li)$	$d(C\cdots Al)$	$d(N_{CN}\cdots Li)$	Π^b
(E)-3	1.275	1.504	1.896	1.958				
(Z)-3	1.276	1.505	1.896	1.957				
(E)-4	1.382	1.362	2.060	1.936	2.537			359.18
(Z)-4	1.377	1.366	2.029	1.967	2.281			359.00
(E)-5	1.309	1.448	2.029		3.227	2.082		342.97
(Z)-5	1.308	1.444	1.924			2.097		334.89
(E)-7	1.259	1.550	1.980	1.940			2.167	
(E)-7b	1.269	1.524	1.910	1.974				
(Z)-7	1.270	1.529	1.908	1.964				
(E,Z)-8	1.361	1.379	2.263	1.945			2.137	358.77
(Z,Z)-8	1.377	1.366	2.114	2.016			2.056	359.74
(E,E)-8	1.388	1.357	1.985	1.981				360.00
(Z,E)-8	1.361	1.378	2.070	1.974	2.330			359.97
(E,Z)-9	1.308	1.447	1.967			2.167		345.25
(Z,Z)-9	1.298	1.463	2.016			2.194		342.92
(E,E)-9	1.303	1.459	2.040			2.123		342.76
(Z,Z)-9	1.294	1.481	1.987			2.090		330.54
19	1.262	1.518	1.724					
(Z)-20	1.349	1.392	1.848		2.128			356.05
(E)-20a	1.353	1.393	1.970		2.169			356.18
(E)-20b	1.379	1.358	1.781					360.00
(Z)-21	1.245	1.622	1.863				2.090	
21b	1.255	1.545	1.737					
(Z,Z)-22	1.336	1.398	1.904				1.985	360.00
(E,Z)-22a	1.331	1.418	2.070		2.267		2.345	359.95
(E,Z)-22b	1.354	1.376	1.802					360.00
(Z,E)-22	1.334	1.406	1.866		2.158			356.44
(E,E)-22a	1.339	1.405	2.008			2.226		357.19
(E,E)-22b	1.357	1.371	1.803					360.00

[a]Bond distances in angstroms. [b]Π is the sum of bond angles at the terminal azaallyl-C in degrees.

Scheme 3. Topologies of Products of LAH Addition to Nitrile RC≡N
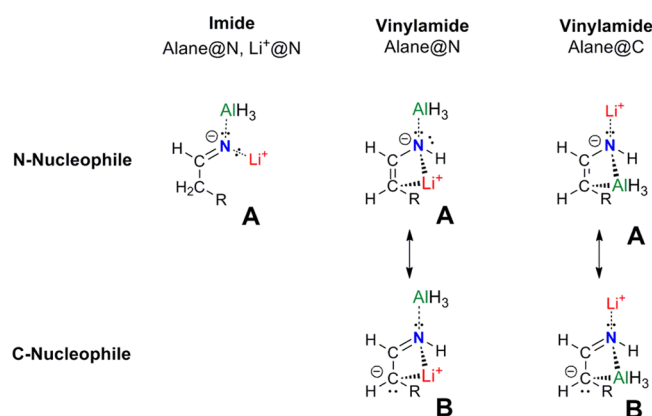
Energies computed with the solvation model SMD and based on the MP2 optimized structures, SMD(MP2/6-311+G*)//MP2/6-311+G* (: = SMD) also are listed in Table S1 (Supporting Information), and imide preference energies $\Delta G' = \Delta E' + (\Delta G - \Delta E)$ are reported in Table 3, where $\Delta E'$ is evaluated with the SMD energies. Energies computed up to the level QCISD(full,T)/6-311++G(2df,2pd) and based on the MP2-optimized structures are collected in the Supporting Information, and imide preference energies $\Delta G'' = \Delta E'' + (\Delta G - \Delta E)$ are reported in Table 3, where $\Delta E''$ is evaluated with the QCISD(full,T)/6-311++G-(2df,2pd)//MP2(full)/6-311+G* (: = QCI) energies. Finally, the imide preference energies $\Delta G''' = \Delta E''' + (\Delta G - \Delta E)$ in column

QCI-SMD of Table 3 are based on the QCI energies $\Delta E''$ and include solvation corrections $\Delta E''' = \Delta E'' + (\Delta E' - \Delta E)$.

■ RESULTS AND DISCUSSION

Nomenclature to Discuss LAH Additions. Mechanistic discussions of LAH reductions of nitriles frequently consider the reaction of AlH_4^- with nitrile (i.e., Scheme 1), and the product of hydride transfer is an imide which binds to or aggregates with alane AlH_3. We include the counterion Li^+ explicitly in all structures as is indicated in Scheme 3. The imide-N is a σ-bidentate Lewis base site (LBS), and we draw dashed bonds in the Lewis structure **A** between the donor-N and the two Lewis acids AlH_3 and Li^+. The aggregation gives rise to isomers about the CN bond and the (E)-isomer is shown in Scheme 3.

The imides can be converted to enamides by 1,3-H-shift. The azaallyl systems are important in discussions of oligomerization reactions because they feature both N- and C-nucleophilic sites. The tautomerization converts the σ-bidentate Lewis base imide-N into the σ-monodentate Lewis base azaallyl-N, and hence, AlH_3 and Li^+ now compete for this σ-LBS and the possibility for coordination isomers must be considered. It is one option to keep the N_σ-coordination of the alane and for lithium cation to engage in π-coordination. It is a second option to keep the N_σ-coordination of the lithium cation and for alane to engage in π-coordination. It is this second option that one might overlook when considering the LAH reduction of a nitrile without explicit consideration of the counterion.

Table 2. Relative and Reaction Energies Computed at the MP2(full)/6-311+G* Level

	parameter	ΔE	ΔH_0	ΔH_{298}	ΔG_{298}
1	isomer pref, E_{rel}, (Z)-**3** vs (E)-**3**	0.25	0.31	0.28	0.21
2	isomer pref, E_{rel}, (Z)-**4** vs (E)-**4**	−6.63	−5.89	−6.18	−5.37
3	isomer pref, E_{rel}, (Z)-**5** vs (E)-**5**	−5.50	−5.94	−5.50	−6.66
4	isomer pref, E_{rel}, (Z)-**5** vs (Z)-**4**	7.53	7.29	7.50	6.78
5	tautomer pref, E_{rel}, (Z)-**4** vs (E)-**3**	−2.01	−0.84	−1.49	0.55
5b				−1.35	−0.14
6	tautomer pref, E_{rel}, (Z)-**5** vs (E)-**3**	5.52	6.45	6.01	7.33
7	addition, E_{rxn}, **1** + **2** → (E)-**3**	−33.64	−29.13	−29.12	−17.91
8	addition, E_{rxn}, **1** + **2** → (Z)-**4**	−35.65	−29.97	−30.62	−17.36
9	addition, E_{rxn}, **1** + **2** → (Z)-**5**	−28.12	−22.68	−23.11	−10.58
10	conf pref, E_{rel}, (E)-**7b** vs (E)-**7**	10.48	10.70	10.85	9.91
11	isomer pref, E_{rel}, (Z)-**7** vs (E)-**7**	9.94	10.11	10.22	9.40
12	isomer pref, E_{rel}, (E,Z)-**8** vs (E,E)-**8**	−4.66	−4.84	−5.00	−4.05
13	isomer pref, E_{rel}, (Z,Z)-**8** vs (Z,E)-**8**	−7.55	−7.41	−7.53	−7.17
14	isomer pref, E_{rel}, (Z,Z)-**8** vs (E,Z)-**8**	−8.21	−7.41	−7.68	−6.98
15	isomer pref, E_{rel}, (E,Z)-**9** vs (E,E)-**9**	1.48	0.92	1.31	0.25
16	isomer pref, E_{rel}, (Z,Z)-**9** vs (Z,E)-**9**	−9.21	−9.19	−9.26	−8.61
17	isomer pref, E_{rel}, (Z,E)-**9** vs (E,Z)-**9**	−15.45	−15.42	−15.43	−15.13
18	isomer pref, E_{rel}, (Z,Z)-**9** vs (Z,Z)-**8**	6.60	6.45	6.37	6.79
19	tautomer pref, E_{rel}, (Z,Z)-**8** vs (E)-**7**	−5.32	−3.83	−4.25	−2.88
20	tautomer pref, E_{rel}, (Z,Z)-**9** vs (E)-**7**	1.28	2.62	2.12	3.91
21	addition, E_{rxn}, **1** + **6** → (E)-**7**	−51.50	−47.17	−47.20	−34.92
22	addition, E_{rxn}, **1** + **6** → (Z,Z)-**8**	−56.83	−51.00	−51.45	−37.83
23	addition, E_{rxn}, **1** + **6** → (Z,Z)-**9**	−50.22	−44.55	−45.08	−31.04
24	aggreg E_{agg}, AlH_3 + Li^+ → Li^+AlH_3	−20.76	−19.18	−19.38	−13.43
25	isomer pref, E_{iso}, C_{3v}-**1b** vs C_{2v}-**1a**	0.61	0.63	0.55	1.56
26	act energy, E_{act}, C_s-**1c** vs C_{2v}-**1a**	1.98	1.68	1.33	2.05
27	E_{CHF}, LiH + AlH_3 → LAH	−51.14	−46.79	−47.63	−39.17
28	dimer, E_{dim}, 2 LiH → $(LiH)_2$	−49.08	−45.55	−46.43	−38.33
29	dimer, E_{dim}, 2 AlH_3 → $(AlH_3)_2$	−33.77	−29.26	−30.04	−20.82
30	E_{DCHF}, $(LiH)_2$ + $(AlH_3)_2$ → $(LAH)_2$	−62.23	−58.64	−58.90	−46.94
31	dimer, E_{dim}, 2 LAH → $(LAH)_2$	−42.79	−39.86	−40.11	−27.75
32	$(LiH)_2$ + 0.5 $(AlH_3)_2$ → **17**	−32.87	−31.12	−31.21	−25.71
33	**17** + 0.5 $(AlH_3)_2$ → $(LAH)_2$	−29.36	−27.52	−27.69	−21.23
34	$(AlH_3)_2$ + 0.5 $(LiH)_2$ → **18**	−27.46	−25.84	−25.79	−20.55
35	**18** + 0.5 $(LiH)_2$ → $(LAH)_2$	−34.78	−32.80	−33.11	−26.39
36	E_{rel}, (E)-**20b** vs (E)-**20a**	−1.41	−1.74	−1.33	−2.42
37	(E)-**20b** vs (Z)-**20**	10.89	10.41	10.62	9.39
38	taut pref, E_{rel}, (Z)-**20** vs **19**	−8.46	−7.52	−8.13	−6.48
39	conf pref, E_{rel}, **21b** vs (Z)-**21**	9.15	9.53	9.83	8.34
40	E_{rel}, (E,Z)-**22b** vs (E,Z)-**22a**	−0.41	−0.64	−0.26	−1.61
41	E_{rel}, (E,E)-**22b** vs (E,E)-**22a**	−6.70	−6.62	−6.34	−7.19
42	(E,Z)-**22b** vs (Z,Z)-**22**	23.01	22.44	22.89	21.34
43	(Z,E)-**22** vs (E,E)-**22b**	−7.15	−6.73	−7.11	−6.01
44	(Z,E)-**22** vs (Z,Z)-**22**	17.73	17.50	17.64	17.21
45	(E,Z)-**22b** vs (E,E)-**22b**	−1.87	−1.79	−1.85	−1.89
46	taut Pref, E_{rel}, (Z,Z)-**22** vs (Z)-**21**	−23.85	−23.85	−22.45	−21.71
47	*anti*-**24b** vs *syn*-**24b**	2.25	2.04	2.12	1.96
48	(*anti,Z*)-**26** vs (*syn,Z*)-**26**	4.57	4.35	4.38	4.34
49	(*anti,E*)-**26** vs (*syn,E*)-**26**	1.51	1.46	1.46	1.47
50	taut pref, E_{rel}, *syn*-**24b** vs **23**	−8.22	−7.63	−7.64	−7.44
51	taut pref, E_{rel}, (*syn,Z*)-**26** vs **25**	−25.50	−23.52	−23.91	−22.57
52	(Z)-**20** → *syn*-**24b** + Li^+	173.22	169.87	170.53	161.88
53	(Z,Z)-**22** → (*syn,Z*)-**26** + Li^+	167.14	164.49	165.02	156.17
54	**2** + LiH → (Z)-**20**	−33.38	−26.73	−27.83	−16.98
55	**2** + **1** → (Z)-**20** + AlH_3	17.76	20.06	19.80	22.19
56	**2** + **1** → (Z)-**20** + 0.5·$(AlH_3)_2$	0.88	5.44	4.78	11.78
57	**2** + **14** → (Z)-**20** + **18**	25.94	28.85	28.50	28.58
58	**2** + **14** → (Z)-**4** + **1**	7.14	9.89	9.50	10.38
59	**2** + **14** → (Z)-**4** + 0.5·**14**	−14.25	−10.04	−10.56	−3.49
60	**6** + LiH → (Z,Z)-**22**	−70.37	−63.27	−64.30	−52.94

Table 2. continued

	parameter	ΔE	ΔH_0	ΔH_{298}	ΔG_{298}
61	**6** + **1** → (Z,Z)-**22** + AlH$_3$	−19.22	−16.47	−16.67	−13.77
62	**6** + **1** → (Z,Z)-**22** + 0.5·(AlH$_3$)$_2$	−36.11	−31.10	−31.69	−24.18
63	**6** + **14** → (Z,Z)-**22** + **18**	−11.05	−7.69	−9.97	−7.39
64	**6** + **14** → (Z,Z)-**8** + **1**	−14.03	−11.14	−11.34	−10.08
65	**6** + **14** → (Z,Z)-**8** + 0.5·**14**	−35.43	−31.07	−31.40	−23.96
66	(Z)-**4** → (Z)-**20** + 0.5 (AlH$_3$)$_2$	36.53	35.41	35.40	29.15
67	(E)-**3** → **19** + 0.5 (AlH$_3$)$_2$	42.98	42.08	42.04	36.17
68	(Z,Z)-**8** → (Z,Z)-**22** + 0.5 (AlH$_3$)$_2$	20.72	19.90	19.77	13.65
69	(E)-**7** → (Z)-**21** + 0.5 (AlH$_3$)$_2$	39.25	38.20	37.97	32.48

[a]All values in kcal/mol. [b]Two digits are given for numerical accuracy at any given theoretical level.

Table 3. Imide Preferences of LAH, LiH, and Hydride Adducts of Acetonitrile and Malononitrile at the MP2(full)/6-311+G* Level, Considering the Effects of Electron Correlation at the QCI Level, and Including SMD Solvation Corrections for Diethyl Ether

			MP2	SMD	QCI	QCI-SMD
adduct	nitrile	parameter	ΔG_{298}	$\Delta G_{298}'$	$\Delta G_{298}''$	$\Delta G_{298}'''$
LAH	AN	(Z)-**4** vs (E)-**3**	0.55	2.23	−0.08	1.60
LAH	MN	(Z,Z)-**8** vs (E)-**7**	−2.88	−1.00	−3.74	−1.86
LiH	AN	(Z)-**20** vs **19**	−6.48	−2.53	−7.52	−3.57
LiH	MN	(Z,Z)-**22** vs (Z)-**21**	−21.71	−18.48	−23.13	−19.90
HA	AN	syn-**24b** vs **23**	−7.44	−4.61	−9.01	−6.18
HA	MN	(syn,Z)-**26** vs **25**	−22.57	−20.63	−25.21	−23.27

[a]All values in kcal/mol. [b]Two digits are given for numerical accuracy at any given theoretical level. [c]See Computational Methods for a definition of theoretical levels.

We use different numbers for coordination isomers. The azaallyl anion gives rise to geometrical isomers with regard to the CN bond and it may also give rise to geometrical isomers about the CC bond if R ≠ H. If both geometrical descriptors are needed, then the first descriptor will apply to the CN bond. We will encounter structures in which the placement of the Lewis acid at the azaallyl-N is neither trans nor cis relative to the CHR group. However, it is always easy to describe the position of the H-atom at N as being either cis or trans relative to the CHR group, respectively, and the CN configuration will then be designated as (E) or (Z), respectively.

Major structural parameters are listed in Table 1 for all the ion pairs discussed and these include the parameter Π, the sum of bond angles at the terminal azaallyl-C. The parameter Π is useful to distinguish between π-coordination (Π ≈ 180°) and σ-coordination (330° < Π < 345°).

LAH Addition to Acetonitrile. The addition of LiAlH$_4$ **1** to acetonitrile, **2** may yield (E)-**3** or (Z)-**3** (Figure 1). The isomers of **3** are basically imides in which the anionic imide-N is stabilized by the Lewis acids AlH$_3$ and Li$^+$. Adduct (E)-**3** formally is the product of cis addition of AlH$_4^-$ to nitrile and Li$^+$ coordinates both to N (1.896 Å) and an alane-H (1.776 Å). Adduct (Z)-**3** can be seen as the product of cis addition of LiH to nitrile. As with (E)-**3**, lithium coordinates both to N (1.896 Å) and an alane-H (1.774 Å) in (Z)-**3**.

Structures **4** and **5** are enamide tautomers of **3**. Alane coordinates the σ-LBS at N and Li$^+$ engages in π-coordination in **4**, and this is as expected for an azaallyl. However, the respective structures with Li$^+$ coordinating the σ-LBS at N and alane engaged in π-coordination do not correspond to minima. The structures (E)-**5** (Π = 343°) and (Z)-**5** (Π = 335°) show that alane prefers σ-donation by the enamide's CH$_2$-carbon over π-donation and that the maintenance of direct contact between the two Lewis acids is important. We did search for a
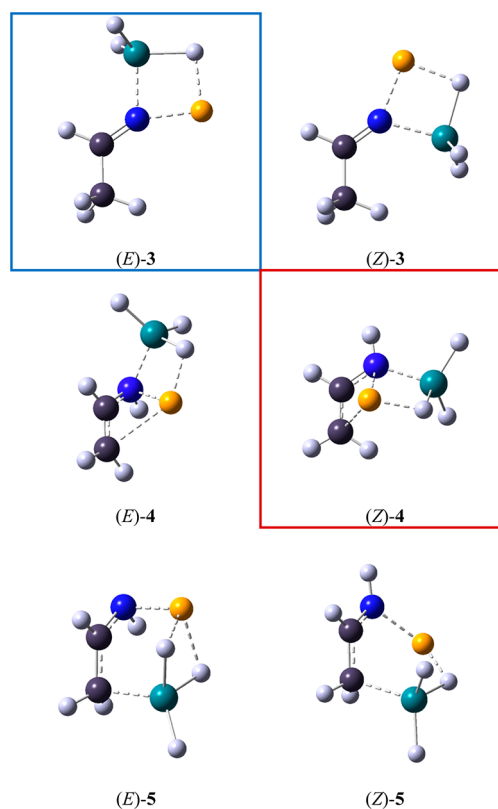
Figure 1. Molecular models of the optimized structures of possible products of LAH addition to acetonitrile. Here and in other figures, the blue frame highlights the best imide species and the red frame shows the best enamide species.
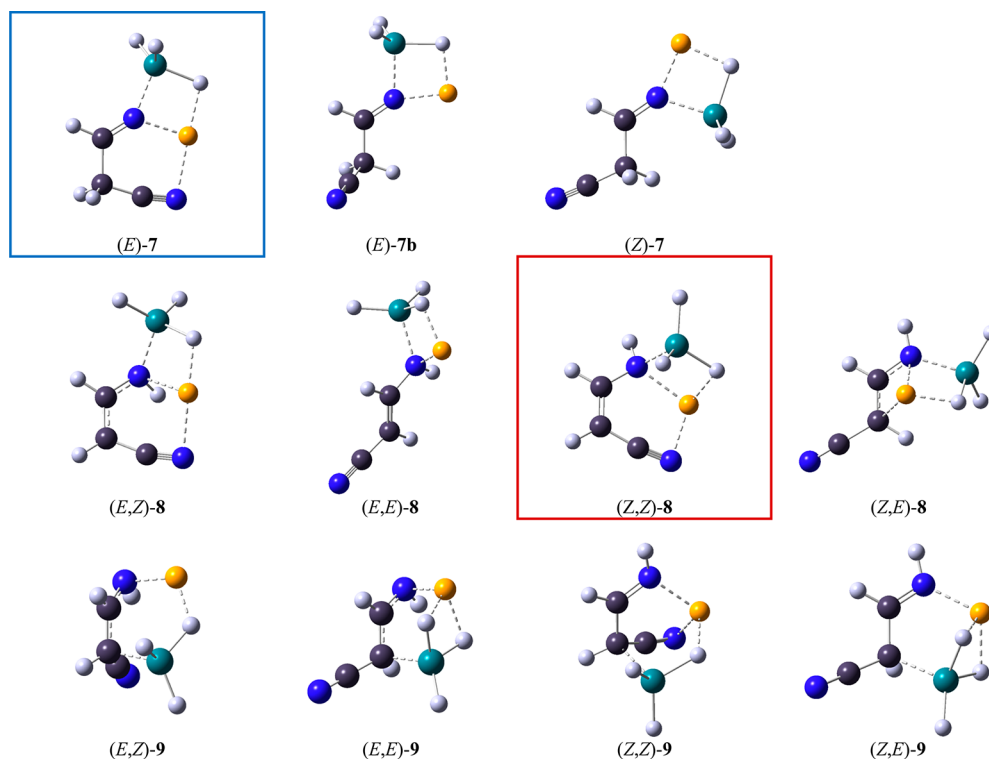
Figure 2. Molecular models of the optimized structures of possible products of LAH addition to malononitrile.

structure of (*E*)-**5** with Li⁺ coordinating the N$_\sigma$-lone pair and alane engaging in π-coordination, and all these attempts led to the (*E*)-**5** structure shown in Figure 1.

The CC bonds in **3** are about 1.50 Å and as expected for a C(sp³)−C(sp²) bond.[34] The CN bonds in **3** are about 1.28 Å and close to imine bonds.[35] The d(CN) and d(CC) values in the tautomers **4** and **5** clearly show that resonance form **A** dominates in **4** whereas the carbanion form **B** dominates in **5**.

There is only a small preference for (*E*)-**3** over (*Z*)-**3** (Table 2, entry 1); both Lewis acids can interact with the imide-N and also with each other. On the other hand, there are very pronounced preferences for the (*Z*)-isomers of **4** and **5** (Table 2, entries 2 and 3) since only the (*Z*)-isomers can optimize the interactions between the Lewis acids and the enamide while maintaining the direct contact between the two Lewis acids. The coordination isomer (*Z*)-**4** is much preferred over (*Z*)-**5**. Most important is the relative stability of the best enamide (*Z*)-**4** compared to the most stable imide (*E*)-**3**, and we find a small preference of ΔG_{298} = 0.55 kcal/mol for the imide aggregate (*E*)-**3** (Table 2, entry 5). Note that the overall binding of (*Z*)-**4** is stronger than in (*E*)-**3**, and it is only for the entropy term that the stability reverses. We also computed the thermochemistry for the temperature of dry ice (−78 °C) and found a small preference of ΔG_{195} = 0.14 kcal/mol for the enamide aggregate (*Z*)-**4** (Table 2, entry 5b).

LAH Addition to Malononitrile. The addition of LiAlH₄ **1** to malononitrile **6** may yield (*E*)-**7** or (*Z*)-**7** (Figure 2). Structures (*E*)-**3** and (*E*)-**7** are similar in the manner in which Li⁺ and AlH₃ coordinate the imide-N and interact with each other. The characteristic new feature in (*E*)-**7** concerns the coordination of the remaining nitrile group by Li⁺. The angles ∠(C−C−C) = 106.6° and ∠(C−C≡N) = 168.5° help to allow for a short contact between the nitrile-N and Li⁺ (2.167 Å). A scan of the potential energy surface of (*E*)-**7** as a

function of the dihedral angle χ = ∠(N═C−CH₂CN) led to the local minimum (*E*)-**7b** (χ = 121.7°), which is about 10 kcal/mol less stable than (*E*)-**7**.

Structures (*Z*)-**3** and (*Z*)-**7** show very similar Li⁺ and AlH₃ coordination of the imide-N and there are no additional interactions with the remaining nitrile. We searched for structures in which the nitrile was placed closer to the alane and all these searches returned to (*Z*)-**7**. To be sure, the potential energy surface of (*Z*)-**7** was scanned as a function of the dihedral angle ∠(N═CCH₂CN), and no additional minimum was found.

Optimization after H/CN replacement in (*E*)-**4** resulted in the structures (*E*,*Z*)-**8** and (*E*,*E*)-**8**, and Li⁺ abandons its π-coordination of the enamide in these structures. Instead, in (*E*,*Z*)-**8** the C−C−N−Al skeleton is twisted by τ = 136.4° such that Li⁺ can coordinate the nitrile-N (2.137 Å) while maintaining its close contact to the amide-N (2.263 Å) and AlH₃ (1.772 Å). The additional nitrile reduces the nucleophilicity of the azaallyl-C and in (*E*,*E*)-**8** the Li⁺ coordinates only the amide-N. Several attempts were made to locate a structure with a π-coordinating Li⁺ but all these tries resulted in (*E*,*E*)-**8**. Optimization after H/CN-replacement in (*Z*)-**4** resulted in (*Z*,*Z*)-**8** and (*Z*,*E*)-**8**. The coordination modes of (*Z*,*E*)-**8** are much like in (*Z*)-**4**. On the other hand, the C−C−N−Al skeleton is twisted by τ = 74.5° in (*Z*,*Z*)-**8** so that Li⁺ can coordinate both the amide-N (2.114 Å) and the nitrile-N (2.056 Å)!

Optimization after H/CN-replacement in (*E*)-**5** resulted in (*E*,*Z*)-**9** and (*E*,*E*)-**9**, and all of these structures share a common mode of coordination of the enamide by the AlH₃·Li⁺ moiety. Optimization after H/CN-replacement in (*Z*)-**5** resulted in the structures (*Z*,*Z*)-**9** and (*Z*,*E*)-**9**. A major structural effect of the additional nitrile group occurs in (*Z*,*Z*)-**9**; the HN−C−C−C skeleton is twisted by τ = 27.2° such that

Li$^+$ can coordinate the nitrile-N (2.194 Å) while maintaining its close contact to the enamide-N (2.016 Å) and one alane-H (1.812 Å).

The presence of the nitrile group in **7** causes a huge preference for (*E*)-**7** over (*Z*)-**7**; ΔG_{298} = 9.40 kcal/mol (Table 2, entry 11). Sets of three relative energies are provided for the isomers of **8** (Table 2, entries 12 - 14) and **9** (entries 15−17). The preferences for the CN-(*Z*)-isomers are ΔG_{298}(**8**) = −7.0 kcal/mol (entry 14) and ΔG_{298}(**9**) = −15.1 kcal/mol (entry 17) and they are enhanced in the malononitrile species compared to the acetonitrile derivatives. As with the acetonitrile systems, there exists a strong preference for **8** over **9** (cf. entries 4 and 18).

Most importantly, there is a clear preference of ΔG_{298} = 2.9 kcal/mol for the enamide aggregate (*Z*,*Z*)-**8** (Table 2, entry 19) over the most stable imide aggregate (*E*)-**7**. This result shows that there is a thermodynamic driving force for tautomerization after the first hydride addition to malononitrile and this driving force exists even at room temperature.

Interactions of Li$^+$ with Neutral and Charged AlH$_n$ Species. All of the products of LAH addition to acetonitrile and malononitrile retain one or two Li$^+$···H−AlH$_2$ contacts. We considered the complex **10** between Li$^+$ and AlH$_3$ to learn about this interaction. Complex **10** is C_{2v}-symmetric (Figure 3) with two Li$^+$···H−Al contacts (1.982 Å), and it is bound by about 13.4 kcal/mol (Table 1, entry 24). The complex **1** (or **1a**) between Li$^+$ and AlH$_4^-$ also is C_{2v}-symmetric (Figure 3) with two Li$^+$···H−Al contacts (1.756 Å). The C_{3v}-symmetric structure **1b** (Figure 3) with three Li$^+$···H−Al contacts (1.921 Å) corresponds to a local minimum, and it is 1.6 kcal/mol less
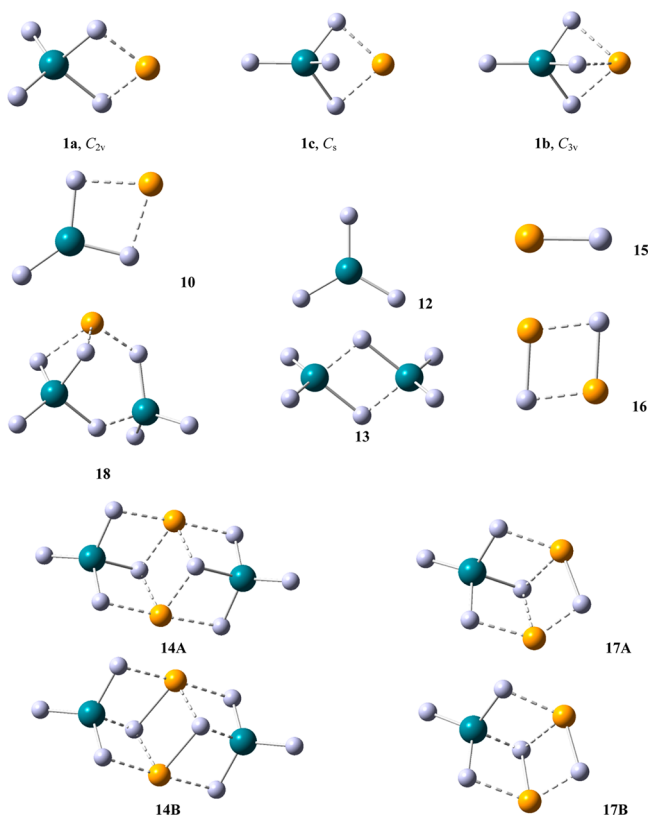
stable than **1a**. The C_s-symmetric transition-state structure **1c** for the isomerization also was located, **1c** (Figure 3), and it is 2.1 kcal/mol above **1a**.

The reaction energy for the complex hydride formation LiH + AlH$_3$ → LiAlH$_4$ is exothermic by about E_{CHF} = −39.2 kcal/mol, and hence, it is essentially impossible to completely separate LiH and AlH$_3$ after they have been mixed. It is for this reason that we are considering the reaction of nitriles with LAH rather than with LiH or AlH$_3$. This remains true if one considers larger aggregates, i.e., the reaction (LiH)$_2$ + (AlH$_3$)$_2$ → (LiAlH$_4$)$_2$ is exergonic by about −46.9 kcal/mol (entry 30, Table 2), although the aggregate formations are less exothermic on a "per LAH" basis. The structure of the dimer (LiAlH$_4$)$_2$, **14** essentially preserves (LiH)$_2$ in its core, i.e. one could think of **14** as (LiH)$_2$·2(AlH$_3$). We also computed the adducts **17**, (LiH)$_2$(AlH$_3$) and **18**, (LiH)(AlH$_3$)$_2$, and the energies of the stepwise formations of the LAH dimer **14** (entries 32−35).

Considering the strength of the Li$^+$···HAlH$_2$ interaction together with the strength of the dative bonding between the parent amide anion and AlH$_3$ (71.1 kcal/mol),[36] one would assume that the AlH$_3$ moiety is strongly bound in an LAH-adduct of a nitrile. We studied the potential energy surface of the LiH adducts of acetonitrile and malononitrile to determine their alane affinities.

LiH Addition to Acetonitrile and Malononitrile. The structure **19** is the primary product of the addition of LiH to acetonitrile (Figure 4), and it features a near-linear (C−N−Li)
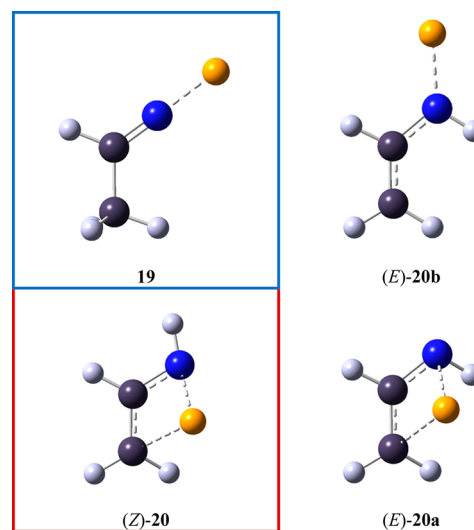
Figure 4. Molecular models of the optimized structures of possible products of LiH addition to acetonitrile.

Figure 3. Molecular models of the optimized structures of the Li$^+$ adduct of AlH$_3$, AlH$_3$ monomer and dimer, and LiAlH$_4$ monomer and dimer.

skeleton, ∠(C−N−Li) = 179.4° with a short lithium contact (1.724 Å). This structure results by optimization of initial structures that correspond to syn and anti addition, respectively. The enamide tautomers (*Z*)-**20** and (*E*)-**20** of **19** are the anti and syn isomers of the lithium enolate[37,38] of acetaldehyde imine, respectively.[39,40] N$_\sigma$-Coordination in (*E*)-**20b** is much preferred over π-coordination in (*E*)-**20a** (entry 36) and the isomer (*Z*)-**20** with its lithium π-coordination is greatly preferred over (*E*)-**20b** (entry 37).

Structure (*Z*)-**21** is the primary product of LiH addition to malononitrile (Figure 5), and it features short contacts between Li$^+$ and the imide-N (1.863 Å) and the nitrile-N
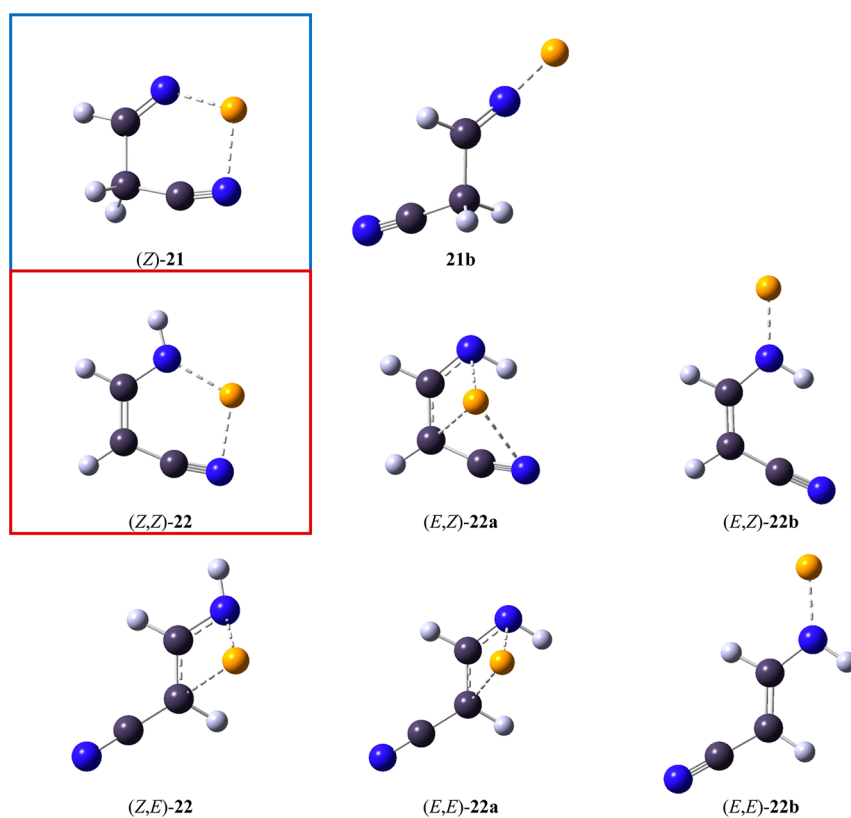
Figure 5. Molecular models of the optimized structures of possible products of LiH addition to malononitrile.
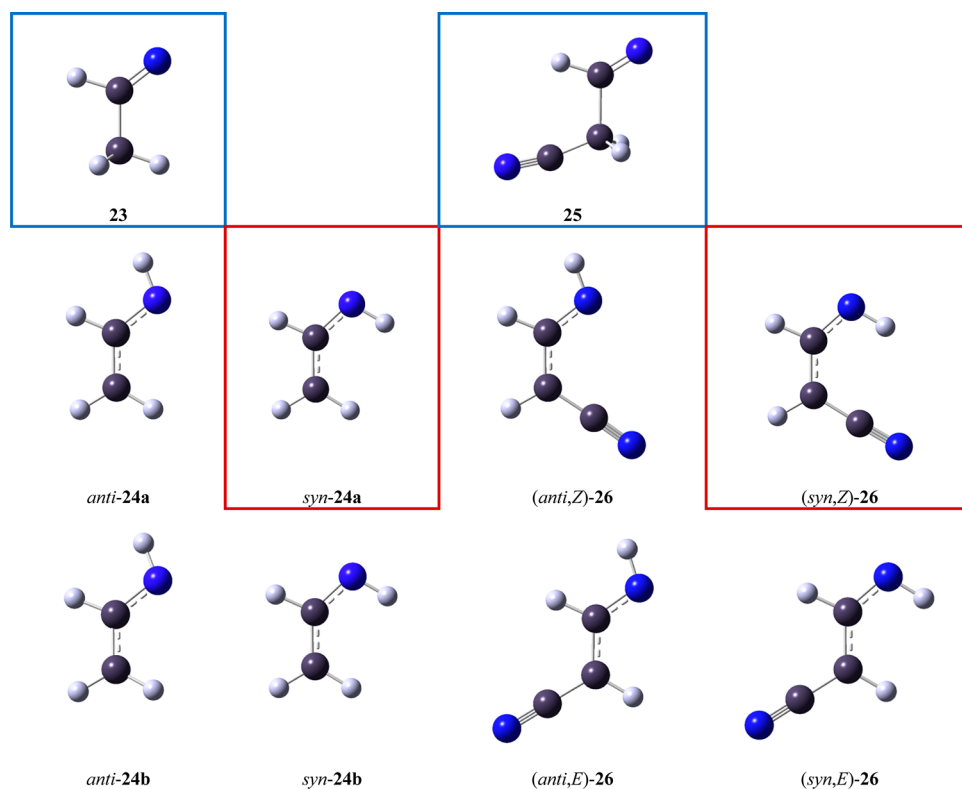
Figure 6. Molecular models of the optimized structures of possible products of hydride addition to acetonitrile and malononitrile.

(2.090 Å). The putative product (*E*)-**21** of cis-addition of LiH to **6**, does not exist as a local minimum and searches for (*E*)-**21** inadvertently led to (*Z*)-**21**. Searches for potential CC-

conformers of either (*Z*)-**21** or (*E*)-**21** resulted in the same local minimum **21b**; a gauche structure with ∠(C−C−C−N) = 123.5° and a near-linear lithium imide fragment with ∠(C−

N−Li) = 175.3°. Structure **21b** is analogous to **19**, but it is much less stable than (Z)-**21** (entry 39). By far, the most stable lithium ion pair of the cyanoenamide tautomer is (Z,Z)-**22** with a lithium coordination similar to (Z)-**20** (Figure 5). The second best isomer of **22** is (Z,E)-**22**, and this structure features π-coordination in analogy to (Z)-**20**. The (E,Z) and (E,E) isomers of **22** can be realized with σ- or π-coordination, and σ-coordination is preferred in both of these isomers (entries 40 and 41).

There is a preference of 6.5 kcal/mol for enamide (Z)-**20** over imide **19** (entry 38) in the lithium ion pair, while there is a preference of ΔG_{298} = 0.6 kcal/mol for imide (E)-**3** over the enamide (Z)-**4** of the LAH adducts. For the malononitrile derivatives, the enamide is preferred in the LiH and LAH adducts but the overwhelming preference in the lithium ion pair is reduced to a few kcal/mol in the LAH adduct: The relative stability of (Z,Z)-**22** with respect to (Z)-**21** is ΔG_{298} = −21.7 kcal/mol (entry 46), and it is much more pronounced than the respective value of ΔG_{298} = −2.9 kcal/mol for the LAH adduct (entry 19, (Z,Z)-**8** vs (E)-**7**).

Hydride Addition to Acetonitrile and Malononitrile. Measurements of the CH acidities of acetonitrile and malononitrile in DMSO give pK_a values of 31.3 and 11.4, respectively,[41−44] and this very large acidity difference should be reflected in the imide−enamide equilibria resulting from hydride addition to nitriles. To assess the latter, one would need to know the NH and CH acidities of the imines HN═CRCH₂X (R = H, X = H, CN). The NH acidities of imines are pK_a ≈ 31.[45] The CH acidities of imines are not well-known, but an estimate is provided by the related carbonyls O═CPhCH₂X (X = H, CN) with their pK_a values of 24.7 (X = H)[46] and 10.2 (X = CN).[47] One would thus expect a strong thermodynamic preference for the enamide over the imide and this preference should be about $\Delta\Delta G$ ≈ 20.5 kcal/mol stronger for the cyano-substituted system because ΔpK_a ≈ 15. We computed the structures of the imides and enamides that result by hydride addition to acetonitrile and malononitrile, respectively, and these are shown in Figure 6. While the planar structures *anti*- and *syn*-**24a** formally are transition-state structures for CH₂-inversion in *anti*- and *syn*-**24b** in their respective extremely low-barrier double-well potentials, the structures of all isomers of **26** are planar. The anions show a *syn*-preference, and it is especially pronounced in the (Z)-**26** because of the intramolecular hydrogen bonding between the imine-NH and the nitrile function (Table 2, entries 47−49).

For the free anions the computations show clear preferences for the enamide over the imide of ΔG_{298} = −7.4 kcal/mol (Table 2, entry 50) and ΔG_{298} = −22.6 kcal/mol (entry 51) for acetonitrile and for malononitrile, respectively. The enamide preferences of the free anions are within 1 kcal/mol of the enamide preferences of the respective lithium ion pairs resulting from LiH addition to acetonitrile (ΔG_{298} = −6.5 kcal/mol, entry 38) and malononitrile (ΔG_{298} = −21.7 kcal/mol, entry 46). Lithium ion pair formation stabilizes both the imide and the enamide very much (entries 52 and 53), but lithium ion pair formation alone does not shift the imide−enamide equilibria in a significant fashion.

LiH vs LAH Addition and Alane Affinities. Several reaction energies listed in Table 2 are relevant to the hydride addition to acetonitrile (entries 54−59) and malononitrile (entries 60−65) using the substrates LiH, LAH, and LAH dimer (**14**), respectively, and considering various aggregation states of the inorganic products.

One important comparison concerns the LiH and LAH additions to each nitrile by way of the reactions "nitrile" + **14** → "best LiH-adduct" + **18** and "nitrile" + 0.5·**14** → "best LAH adduct". Specifically, for acetonitrile we compare the reactions **2** + **14** → (Z)-**20** + **18** (entry 57) and **2** + 0.5·**14** → (Z)-**4** (entry 61, the reaction of **2** and **14** to (Z)-**4** and LAH and considering subsequent dimerization of LAH), and for malononitrile, we compare the reactions **6** + **14** → (Z,Z)-**22** + **18** (entry 63) and **6** + 0.5·**14** → (Z,Z)-**8** (entry 65). This comparison yields three important results: First, there is a strong thermodynamic preference for LAH addition for both nitriles. Second, for acetonitrile only the LAH addition is exergonic. Third, the preference for LAH addition is nearly twice as large for acetonitrile (ca. 32 kcal/mol) than for malononitrile (ca. 16 kcal/mol).

Perhaps the best way to quantify the alane affinity of **20** is by way of the reaction (Z)-**4** → (Z)-**20** + 0.5 (AlH₃)₂; the reaction free energy of the alane dissociation from (Z)-**4** equals the alane affinity of (Z)-**20**. The computed alane affinity is ΔG_{298} = 29.2 kcal/mol (entry 66). Considering the alane affinity of Li⁺ (vide infra), more than half of the alane affinity of **20** is due to dative bonding between enamide and alane. The alane affinity of **19** is somewhat higher (entry 67) and one would expect an imide to be a better Lewis donor compared to an enamide. We determined the alane affinities of (Z,Z)-**22** and (Z)-**21** in analogy (entries 68 and 69) and found the computed alane affinity of (Z,Z)-**22** to be only ΔG_{298} = 13.7 kcal/mol (entry 68), whereas the alane affinity of (Z)-**21** (entry 69) is not too different from that of its analog **19**. The low alane affinity of (Z,Z)-**22** is very similar to the binding energy of a Li⁺···HAlH₂ interaction and, hence, whatever benefit there is due to dative bonding between enamide and alane, it is offset by the weakening of the 1,5-N,N-coordination of the enamide by Li⁺, a weakening that apparently cannot be avoided as alane approaches the enamide-N.

Effects of Higher Level Electron Correlation and Solvation on Imide−Enamide Equilibria. In Table 3 are summarized the pertinent imide preference energies ΔG of the LAH, LiH, and hydride adducts of acetonitrile and malononitrile computed at the level of optimization (MP2-(full)/6-311+G*) together with the imide preference energies computed with the inclusion of the effects of electron correlation at the QCI level, with the inclusion of the effects of ether solvation at the SMD level, and with accounting for both higher level electron correlation and ether solvation at the QCI-SMD level. Solvation benefits the imide ($\Delta G'$ > ΔG) while better electron correlation methods favor the enamide imide ($\Delta G''$ < ΔG), and the combined effects result in modest increases of the imide preference energies ($\Delta G'''$ > ΔG). Importantly, the data in Table 3 show that all the important patterns of the MP2 level data persist. In particular, the data corroborate that most of the intrinsic enamide preference of the free anions is retained in their lithium ion pairs and that the complexation by a second Lewis acid is required to make the imide competitive or even preferred. While lithium enamides are more stable than lithium imides, the enamide preference is greatly reduced in the presence of alane binding so that both tautomers are present at equilibrium. In fact, the computations suggest a small preference for the imide of the LAH adduct of acetonitrile over the enamide. The high alane affinities show that the proper understanding of the LAH reduction requires the consideration of models that include alane and simpler models can lead to wrong conclusions.

Scheme 4. Formation of 3AAN by LAH Addition to Malononitrile and Hypothetical Products of Potential Second Hydride Addition
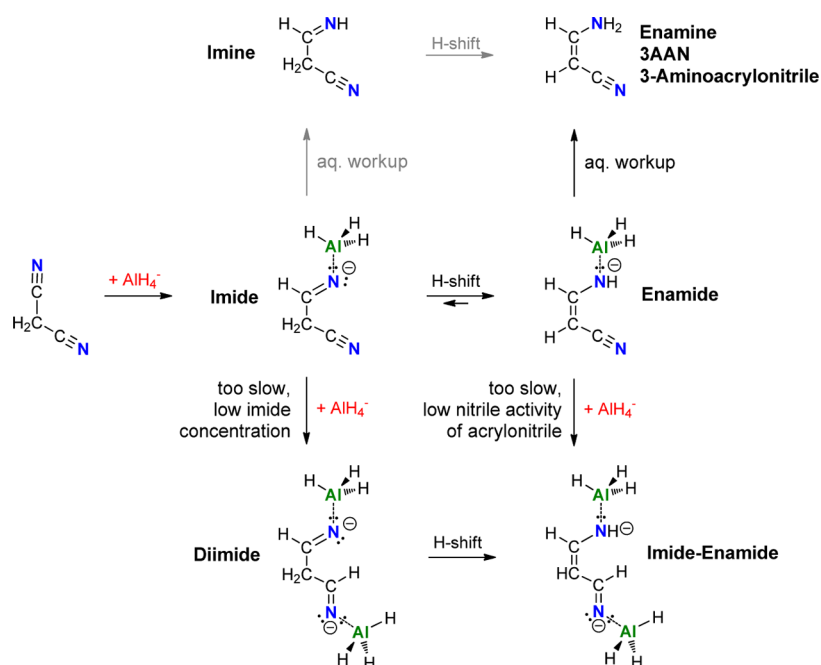
Imide−Enamide Equilibria and Propensity for Further Hydride Reduction.

The hydride reduction chemistry of malononitrile stops at the stage of **7** and/or **8** and products of multiple hydride reduction are not observed. Our results suggest that the imide−enamide equilibria are responsible for the different propensity for second hydride addition of alkyl nitriles as compared to malononitrile.

Consider the second LAH reduction at the *same nitrile group*. Soffer postulated the formation of amide aggregates **1** and/or **2** by second hydride addition to the *imide* produced by the first hydride addition (Scheme 1). Our study shows that the LAH adduct of acetonitrile prefers the imide isomer and (*E*)-**3** is available as substrate for the second hydride addition. On the other hand, LAH addition to malononitrile affords the enamide (*Z,Z*)-**8** and the concentration of imide (*E*)-**7** is too low to sustain a significant rate of reaction for the second hydride addition.

Now consider the putative second LAH reduction of the *intact nitrile group* in the product of the first LAH addition to malononitrile (Scheme 4, bottom half). Scheme 4 shows paths for the addition of an anion to an anion for simplicity, and one must keep in mind that the second addition could be the reaction of neutral LAH with an overall neutral lithium ion pair of an imide or enamide. The major obstacle to the second hydride reduction again concerns the imide-enamide equilibrium and the lack of nitrile activity in the enamide (*Z,Z*)-**8**. Acrylonitriles are substrates for Michael additions[48−50] and the negative charge of the azallyl system further reduces the nitrile's electrophilicity.

Implications for the Mechanism of Reductive Nitrile Dimerization.

The thermodynamic preference for the enamide over the imide tautomer (i.e., **8** vs **7**) or its easy accessibility (i.e., **4** vs **3**) provide for a reasonable mechanistic proposal for the formation of dimeric products. The dimerization begins with the addition of the C-nucleophilic enamide to a nitrile and affords a 1,3-imide-imine. Simple nitriles afford 1,3-imide-imine which can undergo further

reductions and afford diamines (Scheme 1) while the respective dimer of malononitrile leads to pyridine formation. Possible mechanisms for the formation of 2-aminonicotinonitrile **2ANN** are outlined in Scheme 5. Three regions are highlighted that describe the carbanion addition leading to intermediate **C4** (blue), the mechanistic options after *direct* amide addition in **C4** (red), and mechanistic options after amide addition in **C13** (green) *after* **C4** → **C13** *rearrangement*.

Addition of enamide **8** to malononitrile forms the dicyano-substituted imide−imine **C1**. Intermediate **C1** contains four isolated unsaturated functional groups and can stabilize itself to the fully conjugated anion **C4** with two hydrogen transfer reactions (HTR). There are two paths depending as to whether the imide-enamide tautomerization involves a hydrogen from the CH_2 (Type 1) or the CH group (Type 2), respectively, but all paths converge to **C4** after subsequent imine−enamine tautomerization.

The shortest path to pyridine formation involves intramolecular addition of an amide to a nitrile via the sequence **C4** ⇌ **C5** → **C6** → **C7** ⇌ **C8**. Protonation of **C7** or **C8** on workup would provide 4,6-diaminonicotinonitrile (**46DANN**). To affect N-loss, we propose nucleophilic aromatic substitution (S_NAr) of the amino group by hydride.[51−53] Intermediates **C9** and **C10** would result by *ispo*-$S_NAr(H^-, NH_2^-)$ reaction of **C7** or **C8**, respectively, and workup of **C9** and **C10** would afford 6-aminonicotinonitrile (**6ANN**) and/or 4-aminonicotinonitrile (**4ANN**). Since none of these products have been observed experimentally, the shortest route apparently is not taken and one wonders about better, more stable alternatives to **C4** and its rotamer **C5**.

If the 1,3-dinitrile **C4** (or its rotamer **C5**) could rearrange to the 1,1-dinitrile **C12** (or its rotamer **C13**), then one would expect **C13** to lead to 2,4-diaminonicotinonitrile (**24DANN**) and/or 2-aminonicotinonitrile (**2ANN**) and/or 4-aminonicotinonitrile (**4ANN**) in analogy to the paths discussed for **C5**. The rearrangement **C4** → **C12** can be described as a 1,3-formiminyl−nitrile exchange at an allyl anion via the bis-

Scheme 5. Carbanion Attack Mechanism for the Formation of 2,4-Diaminonicotinonitrile (24DANN), 4,6-Diaminonicotinonitrile (46DANN), 2-Aminonicotinonitrile (2ANN), 4-Aminonicotinonitrile (4ANN), and 6-Aminonicotinonitrile (6ANN)
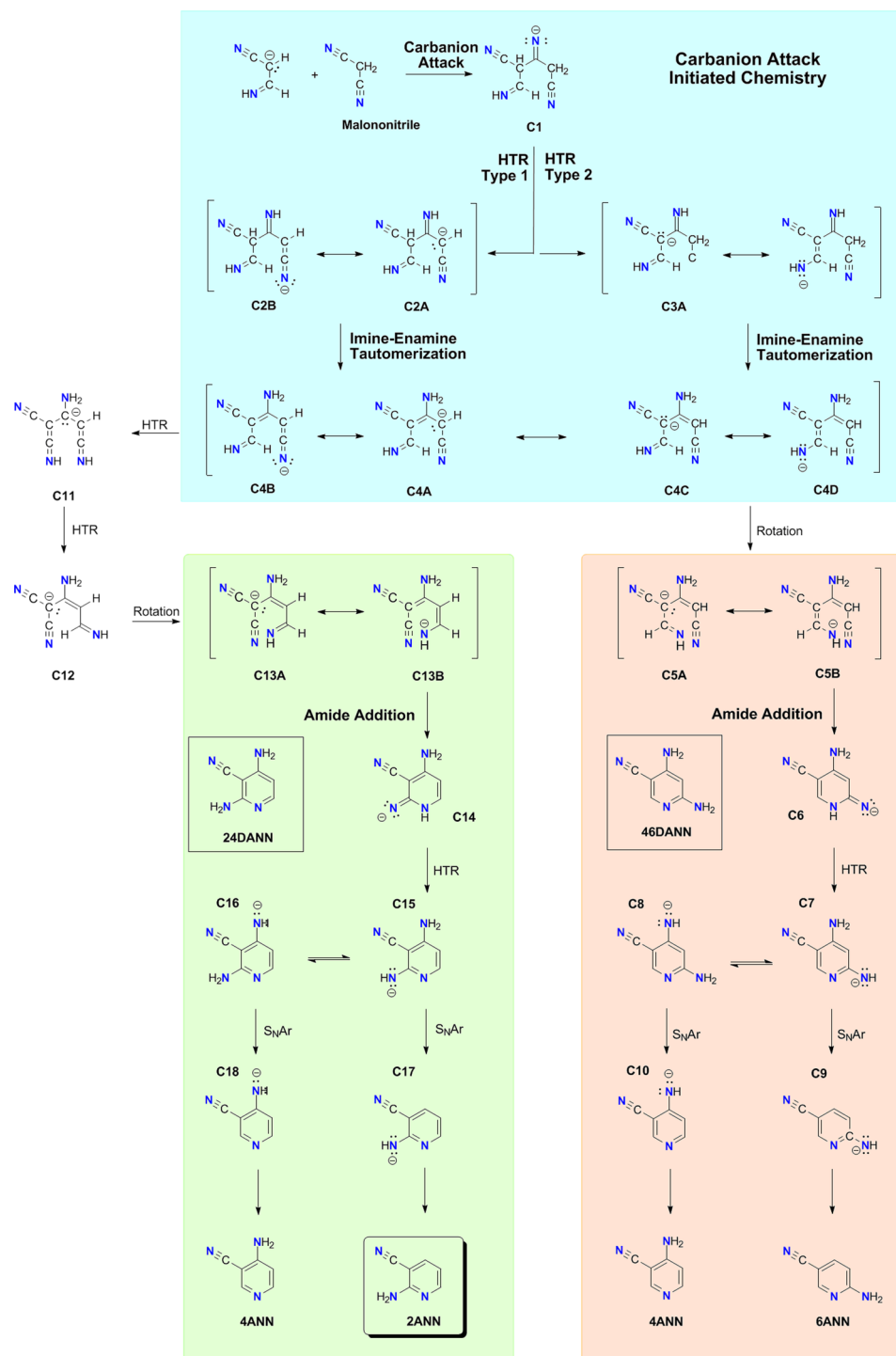
keteneimine species **C11** (Scheme 6) and requires only the *exchange of the oxidation stages of the two functional groups*. The rearrangement involves the successive transfer of two H-atoms, namely symproportionation of **C4** (−CH═NH, −C≡N) to intermediate **C11** with equal oxidation states (two ═C═NH) and subsequent disproportionation to product **C12** (−C≡N, −CH═NH). Both steps involve proton transfers from a formiminyl-CH group to a ketenimide (i.e., **C4B** to **C11B** and **C12B** to **C11C**).

Experimental evidence exists in support of the cyclization **C13 → C14** (Scheme 7). Ege, Frey, and Schuck[54] synthesized 4-dimethylaminobuta-1,3-diene-1,1-dinitrile by coupling of an alkylidenmalodinitrile with $(CH_3)_2N-CHCl_2$ and its reaction with ammonia leads to **2ANN**. Acker and Hamprecht[55] also synthesized the dialkylaminobutadiene-1,1-dinitrile by coupling of malononitrile with $[R_2N═CHCH_2CHCl(OR)]^+Cl^-$. These processes are likely to proceed through the intermediate 4-

Scheme 6. Rearrangement Reaction C4 to C12 (R_1 = CN, R_2 = NH_2, R_3 = H) Exchanges the Oxidation Stages of Two Functional Groups and Can Be Described as a 1,3-Formiminyl−Nitrile Exchange at an Allyl Anion (i.e, C4A → C12A, Allyl Moiety Shaded Green)
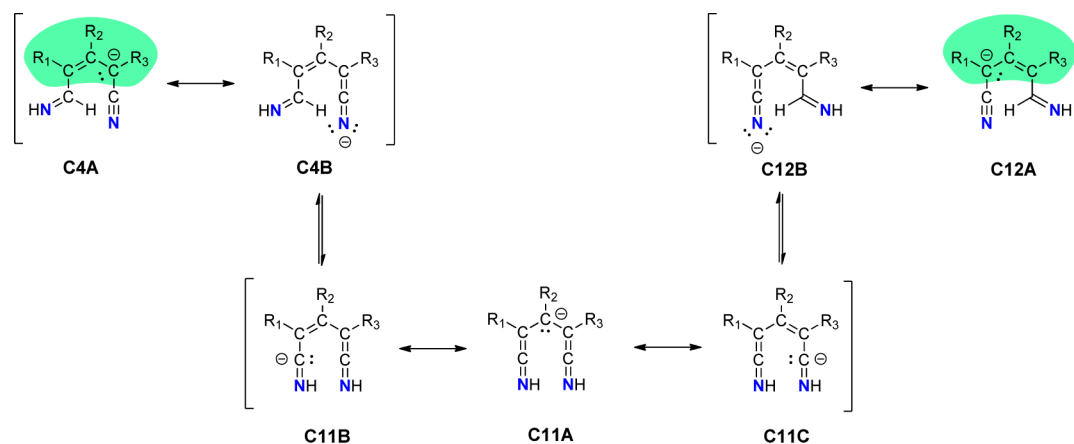
Scheme 7. 4-Aminobutadien-1,1-dinitrile as Intermediate in the Formation of 2-Aminonicotinonitrile (2ANN)
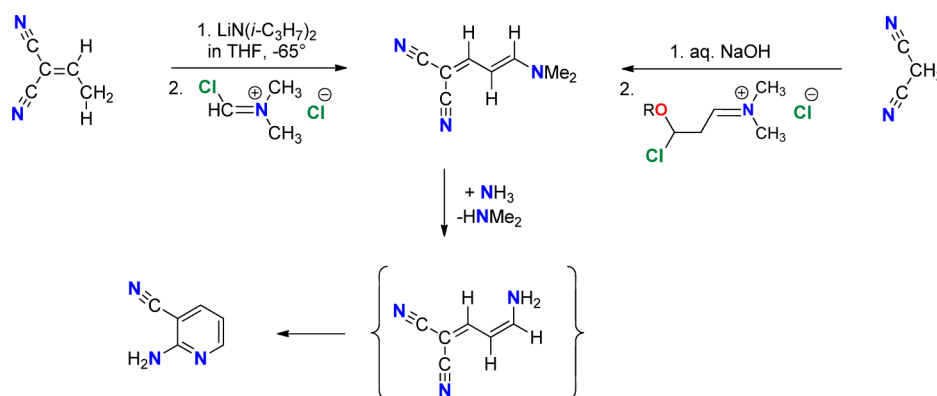
aminobuta-1,3-dien-1,1-dinitrile, and the cyclization **C13** → **C14** involves the 2-amino derivative of the latter.

We also considered plausible reaction paths that begin with an amide-N attack on malononitrile (Scheme S5B, Supporting Information), and that may lead to the formations o **24DANN**, **2ANN**, and **4ANN**. All of these pyridine formations require one carbanion addition to a nitrile and one amide addition to another nitrile, and only one of these can be an intramolecular reaction. Considering the strong complexation of the enamide at nitrogen (i.e., **8**), it seems reasonable to assume a significant advantage for intermolecular carbanion addition to a malononitrile over initial amide-N attack.

■ CONCLUSIONS

The free anions generated by hydride addition to acetonitrile or malononitrile show clear preferences for the enamide over the imide. Lithium ion pair formation stabilizes both tautomers, the localized imide is stabilized slightly more than the enamide, and the enamide preference is somewhat reduced but persists. The alane-complexed lithium ion pairs result in a small imide preference for the LAH adduct of acetonitrile and a *dramatically* reduced enamide preference for the LAH adduct of malononitrile.

The imide-N in $RCH_2CH=N^-$ is a σ-*bi*dentate Lewis base site (SBLBS), and the imide tautomer of the LAH adduct of any nitrile greatly benefits from lithium ion pair formation *and* N→AlH_3 dative bonding and this aggregation can happen

equally well in (*E*)-**3** (R = H) and (*E*)-**7** (R = CN). Hence, the very large reduction of the imide-enamide gap of the malononitrile derivative must reflect less effective aggregation in the enamide. The enamide-NH in the delocalized anion $RCH=CHNH^-$ is a σ-*mono*dentate Lewis base site (SMLBS) which can be occupied either by AlH_3 *or* Li^+. Alane greatly prefers dative bonding with a σ-LBS to π-coordination while lithium ion pairing mostly depends on the distance between the charge centers. Hence, it makes perfect sense that (*Z*)-**4** is the best enamide tautomer of the LAH adduct of acetonitrile. The additional nitrile group in **8** introduces the opportunity for Li^+ to coordinate to both N-atoms in (*Z*,*Z*)-**8**. Alane is not capable of such bridging and becomes relegated to adopt a much less effective coordination mode.

The thermodynamic preference for the enamide over the imide tautomer (i.e., **8** vs **7**) or its easy accessibility (i.e., **4** vs **3**) provide for a reasonable mechanistic proposal for the formation of dimeric products by C−C bond formation by intermolecular enamide addition a nitrile.

Multiple hydride additions occur in the LAH reduction of acetonitrile and requires hydride addition to an imide group. While imide **7** is not the dominant species, this imide is thermodynamically accessible as a reactive intermediate, and the complete lack of second hydride addition of **7** must reflect kinetic factors. On the other hand, the complete absence of additional hydride addition after formation of **C1** is consistent

with the expected isomerization of **C1** to fully conjugated **C4** (Scheme 5).

We proposed a mechanism for the conversion of **C4** to **2ANN** (Scheme 5) that involves the rearrangement of 1,3-dinitrile **C4** to 1,1-dinitrile **C12**, C−N bond formation by intramolecular amide addition to nitrile, NH_2 loss by nucleophilic aromatic substitution by hydride, and protonation on workup. The proposed mechanism is supported by the known formation of **2ANN** from 4-amino-butadien-1,1-dinitrile and by precedent for *ispo*-$S_NAr(H^-, NH_2^-)$ chemistry. The rearrangement of 1,3-dinitrile **C4** to 1,1-dinitrile **C12** is necessitated by the experimentally observed regiochemistry of aminonicotinonitrile formation and the 1,3-formiminyl-nitrile exchange can easily by achieved by double proton transfer (Scheme 6).

In the broader context, our results emphasize that imide-enamide equilibria can be shifted over a wide range by aggregation with several Lewis acids. The aggregation by one cation (ion pair formation) and one neutral Lewis acid (i.e., the alane) provides for very effective stabilization of the imide (two sp^2-LBS). Enamide-NH aggregation with Lewis acids always will be less effective: Either the number of σ-LBS sites at the enamide-NH is reduced (one sp^2-LBS in a delocalized enamide) or the enamide-NH remains σ-bidentate but with σ-LBS sites of diminished quality (two sp^3-LBS in a more or less localized vinyl-amide). The same issues are relevant to and might inform other hydride reductions of nitriles including the nitrile reduction with alkaline metal-free aluminum hydrides (i.e., DIBAL), the hydroboration of nitriles with boranes[56] and borohydrides,[57] boride-mediated nitrile reduction,[58,59] catalytic hydroboration of nitriles,[60] and catalytic hydrosilylation of nitriles.[61]

■ ASSOCIATED CONTENT

Ⓢ Supporting Information

Table of total energies and thermodynamic data computed at the MP2(full)/6-311+G* level, higher level energies up to QCISD(full,T)/6-311++G(2df,2pd)//MP2(full)/6-311+G*, Scheme S5B outlining the formation of pyridines after initial amide-N addition to malononitrile, and Cartesian coordinates of stationary structures. This information is available free of charge via the Internet at http://pubs.acs.org.

■ AUTHOR INFORMATION

Corresponding Author
*E-mail: glaserr@missouri.edu.

Notes
The authors declare no competing financial interest.

■ ACKNOWLEDGMENTS

■ DEDICATION

Dedicated to Professor Andrew Streitwieser, Jr., on the occasion of his 85th birthday.

■ REFERENCES

(1) Harcken, C. *Sci. Synth.* **2006**, *25*, 110−120.

(2) Wünsch, B.; Geiger, C. *Sci. Synth.* **2008**, *40*, 34−37.

(3) Amundsen, L. H.; Nelson, L. S. *J. Am. Chem. Soc.* **1951**, *73*, 242−244.

(4) Soffer, L. M.; Katz, M. *J. Am. Chem. Soc.* **1956**, *78*, 1705−1709.

(5) Soffer, L. M. *J. Org. Chem.* **1957**, *22*, 998−999.

(6) Sieveking, H. U.; Lüttke, W. *Angew. Chem., Int. Ed. Engl.* **1969**, *8*, 458−459.

(7) Taylor, E. C., Jr.; Crovetti, A. J. *J. Org. Chem.* **1954**, *19*, 1633−1640.

(8) Brown, D. J.; Ienega, K. *J. Chem. Soc., Perkin Trans. 1* **1974**, *3*, 372−378.

(9) Kitamura, T.; Okita, M.; Sasaki, Y.; Ishikawa, H.; Fujimoto, A. *Spectrochim. Acta* **2008**, *A69*, 350−360.

(10) Benidar, A.; Guillemin, J.; Mó, O.; Yáñez, M. *J. Phys. Chem. A* **2005**, *109*, 4705−4712.

(11) Mó, O.; Yáñez, M.; Guillemin, J. *ARKIVOC* **2005**, *9*, 239−252.

(12) The (Z)-isomer is more stable than the (E)-isomer with an isomer preference energy of $\Delta G_{298} = 2.0$ kcal/mol at the MP2(full)/6-31G* level: Wu, H.; Glaser, R. *Chem. Res. Toxicol.* **2005**, *18*, 111−114.

(13) Rayat, S.; Qian, M.; Glaser, R. *Res. Toxicol.* **2005**, *18*, 1211−1218.

(14) (a) Coyle, S.; Glaser, R. *J. Org. Chem.* **2011**, *76*, 3987−3996. (b) Glaser, R.; Yin, J.; Miller, S. *J. Org. Chem.* **2010**, *75*, 1132−1142.

(15) Sako, M. *Sci. Synth.* **2004**, *16*, 1155−1267.

(16) Spitzner, D. *Sci. Synth.* **2004**, *15*, 11ff.

(17) Cramer, C. J. *Essentials of Computational Chemistry: Theories and Models*, 2nd ed.; Wiley: Chichester, 2004.

(18) Shavitt, I.; Bartlett, R. J. *Many-Body Methods in Chemistry and Physics: MBPT and Coupled-Cluster Theory*; Cambridge University Press: Cambridge, UK, 2009.

(19) Pople, J. A. *Rev. Modern Phys.* **1999**, *71*, 1267−1274.

(20) Wilson, S. *Handb. Mol. Phys. Quantum Chem.* **2003**, *2*, 314−373.

(21) (a) Krishnan, R.; Binkley, J. S.; Seeger, R.; Pople, J. A. *J. Chem. Phys.* **1980**, *72*, 650−654. (b) Curtiss, L. A.; Binning, R. C., Jr. *Int. J. Quant. Chem.* **1991**, *40*, 781−787.

(22) (a) Pople, J. A.; Head-Gordon, M.; Raghavachari, K. *J. Chem. Phys.* **1987**, *87*, 5968−5975. (b) Pople, J. A. *Nobel Lecture: Quantum Chemical Models. Rev. Mod. Phys.* **1999**, *71*, 1267−1274.

(23) Frisch, M. J.; Pople, J. A.; Binkley, J. S. *J. Chem. Phys.* **1984**, *80*, 3265−3269.

(24) Lynch, B. J.; Truhlar, D. G. *ACS Symp. Series* **2007**, *958*, 153−167.

(25) Curtiss, L. A.; Redfern, P. C.; Raghavachari, K. *J. Chem. Phys.* **2007**, *127*, 124105/1−124105/8 and references cited therein.

(26) Montgomery, J. A., Jr.; Frisch, M. J.; Ochterski, J. W.; Petersson, G. A. *J. Chem. Phys.* **2000**, *11*, 6532−6542.

(27) (a) Cancès, E.; Mennucci, B.; Tomasi, J. *J. Chem. Phys.* **1997**, *107*, 3032−3041.

(28) (a) Tomasi, J.; Cappelli, C.; Mennucci, B.; Cammi, R. From Molecular Electrostatic Potentials to Solvation Models and Ending with Biomolecular Photophysical Processes. In *Quantum Biochemistry*, 1st ed.; Matta, C. F., Ed.; Wiley-VCH: Weinheim, 2010; pp 131−170. (b) Tomasi, J. Modern Theories of Continuum Models: The Physical Model. In *Continuum Solvation Models in Chemical Physics: From Theory to Application*, 1st ed.; Mennucci, B.; Cammi, R., Eds.; John Wiley & Sons Ltd.: West Sussex, 2007; pp 1−28.

(29) (a) Wahlin, P.; Schimmelpfennig, B.; Wahlgren, U.; Grenthe, I.; Vallet, V. *Theor. Chem. Acc.* **2009**, *124*, 377−384. (b) Kongsted, J.; Mennucci, B. *J. Phys. Chem. A* **2007**, *111*, 9890−9900. (c) Jensen, L.; van Duijnen, P. Th. The Discrete Solvent Reaction Field Model: A Quantum Mechanics/Molecular Mechanics Model for Calculating Nonlinear Optical Properties of Molecules in Condensed Phase. In *Atoms, Molecules and Clusters in Electric Fields. Theoretical Approaches to the Calculation of Electric Polarizability*, 1st ed.; Maroulis, G., Ed.; Imperial College Press: London, 2006; pp 283−325.

(30) (a) Ribeiro, R. F.; Marenich, A. V.; Cramer, C. J.; Truhlar, D. G. *J. Comput.-Aided Mater.* **2010**, *24*, 317−333. (b) Marenich, A. V.; Cramer, C. J.; Truhlar, D. G. *J. Phys. Chem. B* **2009**, *113*, 6378−6396.

(c) Marenich, A. V.; Cramer, C. J.; Truhlar, D. G. *J. Phys. Chem. B* **2009**, *113*, 4538−4543.

(31) (a) Halim, M. A.; Shaw, D. M.; Poirier, R. A. *THEOCHEM* **2010**, *960*, 63−72. (b) Saielli, G. *J. Phys. Chem. A* **2010**, *114*, 7261−7265. (c) Smiechowski, M. *Chem. Phys. Lett.* **2010**, *501*, 123−129. (d) Sutton, C. C. R; Franks, G. V.; da Silva, G. *J. Phys. Chem. B* **2012**, *116*, 11999−12006. (e) Acosta-Silva, C.; Bertran, J.; Branchadell, V.; Oliva, A. *J. Am. Chem. Soc.* **2012**, *134*, 5817−5831.

(32) Gaussian 09, Rev. A.1: Frisch, M. J.; Trucks, G. W.; Schlegel, H. B.; Scuseria, G. E.; Robb, M. A.; Cheeseman, J. R.; Scalmani, G.; Barone, V.; Mennucci, B.; Petersson, G. A; Nakatsuji, H.; Caricato, M.; Li, X.; Hratchian, H. P.; Izmaylov, A. F.; Bloino, J.; Zheng, G.; Sonnenberg, J. L.; Hada, M.; Ehara, M.; Toyota, K.; Fukuda, R.; Hasegawa, J.; Ishida, M.; Nakajima, T.; Honda, Y.; Kitao, O.; Nakai, H.; Vreven, T.; Montgomery, J. A., Jr.; Peralta, J. E.; Ogliaro, F.; Bearpark, M.; Heyd, J. J.; Brothers, E.; Kudin, K. N.; Staroverov, V. N.; Kobayashi, R.; Normand, J.; Raghavachari, K.; Rendell, A.; Burant, J. C.; Iyengar, S. S.; Tomasi, J.; Cossi, M.; Rega, N.; Millam, N. J.; Klene, M.; Knox, J. E.; Cross, J. B.; Bakken, V.; Adamo, C.; Jaramillo, J.; Gomperts, R.; Stratmann, R. E.; Yazyev, O.; Austin, A. J.; Cammi, R.; Pomelli, C.; Ochterski, J. W.; Martin, R. L.; Morokuma, K.; Zakrzewski, V. G.; Voth, G. A.; Salvador, P.; Dannenberg, J. J.; Dapprich, S.; Daniels, A. D.; Farkas, Ö.; Foresman, J. B.; Ortiz, J. V.; Cioslowski, J.; Fox, D. J. Gaussian, Inc., Wallingford, CT, 2009.

(33) GaussView 5.0.8: Dennington, R.; Keith, T.; Millam, J. Semichem Inc., Shawnee Mission, KS, 2009.

(34) Kowalczyk, P.; Gauden, P. A.; Terzyk, A. P. *RSC Adv.* **2012**, *2*, 4292−4298.

(35) Pyykkö, P.; Atsumi, M. *Chem.—Eur. J.* **2009**, *15*, 12770−12779.

(36) A study of alane affinities of amides will be reported separately. For the reaction $NH_2^- + 0.5\ (AlH_3)_2 \rightarrow [H_2N{\rightarrow}AlH_3]^-$, the reaction energies are $\Delta E = -76.48$, $\Delta H_0 = -74.83$, $\Delta H_{298} = -75.21$, and $\Delta G_{298} = -71.07$ kcal/mol.

(37) (a) Streitwieser, A. *J. Mol. Modeling* **2006**, *12*, 673−680. (b) Pratt, L. M.; Streitwieser, A. *J. Org. Chem.* **2003**, *68*, 2830−2838. (c) Abbotto, A.; Streitwieser, A. *J. Am. Chem. Soc.* **1995**, *117*, 6358−6359.

(38) (a) Liou, L. R.; McNeil, A. J.; Ramirez, A.; Toombes, G. E. S.; Gruver, J. M.; Collum, D. B. *J. Am. Chem. Soc.* **2008**, *130*, 4859−4868. (b) Godenschwager, P. F.; Collum, D. B. *J. Am. Chem. Soc.* **2008**, *130*, 8726−8732.

(39) (a) Glaser, R.; Streitwieser, A., Jr. *J. Org. Chem.* **1991**, *56*, 6612−24. (b) Glaser, R.; Hadad, C.; Wiberg, K. B.; Streitwieser, A. *J. Org. Chem.* **1991**, *56*, 6625−6637.

(40) (a) Glaser, R.; Streitwieser, A., Jr. *J. Am. Chem. Soc.* **1987**, *109*, 1258−1260. (b) Glaser, R.; Streitwieser, A., Jr. *J. Am. Chem. Soc.* **1989**, *111*, 7340−7348. (c) Glaser, R.; Streitwieser, A., Jr. *J. Am. Chem. Soc.* **1989**, *111*, 8799−8809. (d) Glaser, R.; Streitwieser, A., Jr. *J. Org. Chem.* **1989**, *54*, 5491−5502.

(41) Matthews, W. S.; Bares, J. E.; Bartmess, J. E.; Bordwell, F. G.; Cornforth, F. J.; Drucker, G. E.; Margolin, Z.; McCallum, R. J.; McCollum, G. J.; Vanier, N. R. *J. Am. Chem. Soc.* **1975**, *97*, 7006−7014.

(42) Reich, H. J. Bordwell pK_a Table (Acidity in DMSO), URL: http://www.chem.wisc.edu/areas/reich/pkatable/ (accessed Aug 27, 2012).

(43) Hojatti, M.; Kresge, A. J.; Wang, W. H. *J. Am. Chem. Soc.* **1987**, *109*, 4023−4028.

(44) Talvik, A.; Pihl, A.; Timotheus, H.; Osa, A.; Viira, J.; Timotheus, V. *Reakts. Sposobn. Org. Soedin.* **1975**, *12*, 133−140.

(45) Bordwell, F. G.; Ji, G. Z. *J. Am. Chem. Soc* **1991**, *113*, 8398−8401.

(46) Bordwell, F. G. *Acc. Chem. Res.* **1988**, *21*, 456−463.

(47) Bordwell, F. G.; Van der Puy, M.; Vanier, N. R. *J. Org. Chem.* **1976**, *41*, 1883−1886.

(48) Castonguay, A.; Spasyuk, D. M.; Madern, N.; Beauchamp, A. L.; Zargarian, D. *Organometallics* **2009**, *28*, 2134−2141.

(49) (a) Ma, Y.; Xu, J. *Synthesis* **2012**, *44*, 2225−2230. (b) Cespedes-Camacho, I. F.; Manso, J. A.; Gonzalez-Jimenez, M.; Casado, E. C. J. *Monatsh. Chem.* **2012**, *143*, 723−727.

(50) Ranu, B. C.; Samanta, S. *Tetrahedron* **2003**, *59*, 7901−7906.

(51) Gallardo, I.; Guirado, G.; Marquet, J. *J. Org. Chem.* **2002**, *67*, 2548−2555.

(52) van Gestel, J.; Dujardin, C.; Mauge, F.; Duchet, J. C. *J. Catal.* **2001**, *202*, 78−88.

(53) Rose-Munch, F.; Gagliardini, V.; Renard, C.; Rose, E. *Coord. Chem. Rev.* **1998**, *178−180*, 249−268.

(54) Ege, G.; Frey, H. O.; Schuck, E. *Synthesis* **1979**, *5*, 376−378.

(55) Acker, R. D.; Hamprecht, G. Butadiene dinitriles. *Eur. Pat. Appl.* EP57363 A119820811, 1982.

(56) Wünsch, B.; Geiger, C. *Sci. Synth.* **2008**, *40*, 38−40.

(57) Wünsch, B.; Geiger, C. *Sci. Synth.* **2008**, *40*, 41−43.

(58) (a) Caddick, S.; Judd, D. B.; Lewis, A. K. de K.; Reich, M. T.; Williams, M. R. V. *Tetrahedron* **2003**, *59*, 5417−2423. (b) Khurana, J. M.; Kukreja, G. *Synth. Commun.* **2002**, *32*, 1265−1269.

(59) Osby, J. O.; Heinzman, S. W.; Ganem, B. *J. Am. Chem. Soc.* **1984**, *108*, 67−72.

(60) Khalimon, A. Y.; Farha, P.; Kuzmina, L. G.; Nikonov, G. I. *Chem. Commun.* **2012**, *48*, 455−457.

(61) Gutsulyak, D. V.; Nikonov, G. I. *Angew. Chem., Int. Ed.* **2010**, *49*, 7553−7556.